KA–TP–7–1999

ELECTROWEAK PRECISION DATA AND PRECISION TESTS OF THE SM AND MSSM *

W. Hollik

Institut für Theoretische Physik
Universität Karlsruhe
D-76128 Karlsruhe, Germany

Abstract. These lectures give an overview of the status of radiative correction calculations to provide accurate theoretical predictions for testing the standard model (SM) in present and future experiments. The status of the standard model is discussed in the light of the recent electroweak precision data for the vector boson masses and for the Z resonance observables. As a theoretically well motivated example of physics beyond the SM, the minimal supersymmetric standard model (MSSM) is considered, reviewing precision tests of the MSSM and precise calculations for the mass of the lightest Higgs boson.

*) Lectures given at the 8th Mexican School on Particles and Fields, Oaxaca, Mexico, November 1998. Published in AIP Conference Proceedings 490, Melville, New York 1999, eds. J.C. D'Olivo, G. López Castro, M. Mondragón

Electroweak Precision Data and Precision Tests of the SM and MSSM

W. Hollik

Institut für Theoretische Physik, Universität Karlsruhe
D-76128 Karlsruhe, Germany

Abstract. These lectures give an overview of the status of radiative correction calculations to provide accurate theoretical predictions for testing the standard model (SM) in present and future experiments. The status of the standard model is discussed in the light of the recent electroweak precision data for the vector boson masses and for the Z resonance observables. As a theoretically well motivated example of physics beyond the SM, the minimal supersymmetric standard model (MSSM) is considered, reviewing precision tests of the MSSM and precise calculations for the mass of the lightest Higgs boson.

INTRODUCTION

The e^+e^- colliders LEP and the SLC, in operation since summer 1989, have collected an enormous amount of electroweak precision data on Z and W bosons [1,2]. The W boson properties have in parallel been determined at the $p\bar{p}$ collider Tevatron with a constant increase in accuracy [2,3]; after the discovery of the top quark there [4], its mass has been measured [5] with a precision of better than 3%, to 173.8 ± 5.0 GeV. The ongoing experiments at LEP 2 and the near-future Tevatron upgrade will also, in the coming years, support us with further increases in precision, in particular on the mass of the W and the top, and the SLC might continue to improve the impressive accuracy already obtained in the electroweak mixing angle. This stimulating experimental program together with the theoretical activities to provide accurate predictions from the standard model have formed the era of electroweak precision tests and will keep it alive also in the next years.

The standard theory of the electroweak interaction is a gauge-invariant quantum field theory with the symmetry group SU(2)×U(1) spontaneously broken by the Higgs mechanism. The possibility to perform perturbative calculations for observable quantities in terms of a few input parameters is substantially based on the renormalizability of this class of theories [6]. A certain set of input parameters has to be taken from experiment. In the electroweak standard model essentially three free parameters are required to describe the gauge bosons $\gamma, W^\pm, Z$, and their interactions with the fermions. For a comparison between theory and experiment, hence, three independent experimental input data are required. The most natural choice consists of the electromagnetic fine structure constant α, the muon decay constant (Fermi constant) G_μ, and the mass of the Z boson, which has meanwhile been measured with the same accuracy as the Fermi constant [1,2]. Other measurable quantities are predicted in terms of the input data. Each additional precision experiment, which allows the detection of small deviations from the lowest-order predictions, can be considered a test of the electroweak theory at the quantum level. In the Feynman graph expansion of the scattering amplitude for a given process the higher-order terms show up as diagrams containing closed loops. The renormalizability of the standard model ensures that it retains its predictive power also in higher orders. The higher-order terms are the quantum effects of the electroweak theory. They are complicated in their concrete form, but they are finally the consequence of the basic Lagrangian with a simple structure. The quantum corrections (radiative corrections) contain the self-coupling of the vector bosons as well as their interactions with the Higgs field and the top quark, and provide the theoretical basis for electroweak precision tests. Assuming the validity of the standard model, the presence of the top quark and the Higgs boson in the loop contributions to electroweak observables allows an indirect probe of their mass ranges from comparison with precision data.

The generation of high-precision experiments hence imposes stringent tests on the standard model. A primordial step strengthening our confidence in the standard model has been the discovery of the top quark at the Tevatron [4], at a mass that agrees with the mass range obtained indirectly, through the radiative corrections. Moreover, with the top mass as an additional precise experimental data point one can now fully exploit the virtual sensitivity to the Higgs mass.

The experimental sensitivity in the electroweak observables, at the level of the quantum effects, requires the highest standards on the theoretical side as well. A sizeable amount of work has contributed, over the recent years, to a steadily rising improvement of the standard model predictions, pinning down the theoretical uncertainties to the level required for the current interpretation of the precision data. The availability of both highly accurate measurements and theoretical predictions, at the level of 0.1% precision and better, provides tests of the quantum structure of the standard model, thereby probing its still untested scalar sector, and simultaneously accesses alternative scenarios such as the supersymmetric extension of the standard model.

The lack of direct signals from new physics beyond the standard model makes the high-precision experiments a unique tool also in the search for indirect effects: through possible deviations of the experimental results from the theoretical predictions of the minimal standard model. Since such deviations are expected to be small, it is decisive to have the standard loop effects in the precision observables under control.

These lectures contain a discussion of the theoretical developments for testing the electroweak theory, the status of the standard model in view of the recent precision data, and the implications for the Higgs boson. Precision tests of the MSSM are also discussed, as well as a precise prediction for the mass of the lightest Higgs boson in the MSSM.

STATUS OF PRECISION CALCULATIONS

Radiative corrections entries

The possibility of performing precision tests is based on the formulation of the standard model as a renormalizable quantum field theory preserving its predictive power beyond tree-level calculations. With the experimental accuracy being sensitive to the loop-induced quantum effects, also the Higgs sector of the standard model is being probed. The higher-order terms induce the sensitivity of electroweak observables to the top and Higgs mass m_t, M_H and to the strong coupling constant α_s.

The calculation of electroweak observables in higher orders requires the concept of renormalization to get rid of the divergences in the Feynman integral evaluation and to define the physical input parameters. In QED and in the electroweak theory the classical Thomson scattering and the particle masses set natural scales where the parameters $e = \sqrt{4\pi\alpha}$ and the electron, muon, ... masses can be defined. In the electroweak standard model a distinguished set for parameter renormalization is given in terms of e, M_Z, M_W, M_H, m_f with the masses of the corresponding particles. The finite parts of the counter terms are fixed by the renormalization conditions that the propagators have poles at their physical masses, and e becomes the $ee\gamma$ coupling constant in the Thomson limit of Compton scattering. This electroweak on-shell scheme, the extension of the familiar QED renormalization, has been used in many practical applications [7]– [17]. The mass of the Higgs boson, as long as it is experimentally unknown, is treated as a free input parameter. In practical calculations, the W mass is replaced by G_μ as an input parameter by using relation (18).

Instead of the set e, M_W, M_Z as basic free parameters other renormalization schemes make use of α, G_μ, M_Z [18] or perform the loop calculations in the $\overline{MS}$ scheme [19]– [22]. Other schemes applied in the past utilize the parameters α, G_μ, $\sin^2\theta_W$, with the mixing angle deduced from neutrino-electron scattering [23], or the concept of effective running couplings [24,25].

Before predictions can be made from the theory, a set of independent parameters has to be taken from experiment. For practical calculations the physical input quantities α, G_μ, M_Z, m_f, M_H, α_s are commonly used to fix the free parameters of the standard model. Differences between various schemes are formally of higher order than the one under consideration. The study of the scheme dependence of the perturbative results, after improvement by resummation of the leading terms, allows us to estimate the missing higher-order contributions.

Related to charge and mass renormalization, there occur two sizeable effects in the electroweak loops that deserve a special discussion:

(i) Charge renormalization and light fermion contribution:

Charge renormalization introduces the concept of electric charge for real photons ($q^2 = 0$) to be used for the calculation of observables at the electroweak scale set by M_Z. Hence the difference

$$\mathrm{Re}\,\hat{\Pi}^{\gamma}(M_Z^2)) = \mathrm{Re}\,\Pi^{\gamma}(M_Z^2) - \Pi^{\gamma}(0) \tag{1}$$

of the photon vacuum polarization is a basic entry in the predictions for electroweak precision observables. The purely fermionic contributions correspond to standard QED and do not depend on the details of the electroweak theory. They are conveniently split into a leptonic and a hadronic contribution

$$\mathrm{Re}\,\hat{\Pi}^{\gamma}(M_Z^2)_{\mathrm{ferm}} = \mathrm{Re}\,\hat{\Pi}^{\gamma}_{\mathrm{lept}}(M_Z^2) + \mathrm{Re}\,\hat{\Pi}^{\gamma}_{\mathrm{had}}(M_Z^2)\,, \tag{2}$$

where the top quark is not included in the hadronic part (5 light flavours); it yields a small non-logarithmic contribution

$$\hat{\Pi}^{\gamma}_{\mathrm{top}}(M_Z^2) \simeq \frac{\alpha}{\pi}\, Q_t^2\, \frac{M_Z^2}{5\, m_t^2} \simeq 0.6 \cdot 10^{-4}\,. \tag{3}$$

The quantity

$$\begin{aligned} \Delta\alpha &= \Delta\alpha_{\mathrm{lept}} \;+\; \Delta\alpha_{\mathrm{had}} \\ &= -\,\mathrm{Re}\,\hat{\Pi}^{\gamma}_{\mathrm{lept}}(M_Z^2) - \;\mathrm{Re}\,\hat{\Pi}^{\gamma}_{\mathrm{had}}(M_Z^2) \end{aligned} \tag{4}$$

corresponds to a QED-induced shift in the electromagnetic fine structure constant

$$\alpha \;\rightarrow\; \alpha(1 + \Delta\alpha)\,, \tag{5}$$

which can be resummed according to the renormalization group accommodating all the leading logarithms of the type $\alpha^n \log^n(M_Z/m_f)$. The result can be interpreted as an effective fine structure constant at the Z mass scale:

$$\alpha(M_Z^2) \;=\; \frac{\alpha}{1 - \Delta\alpha}\,. \tag{6}$$

It corresponds to a resummation of the iterated 1-loop vacuum polarization from the light fermions to all orders.

$\Delta\alpha$ is an input of crucial importance because of its universality and of its remarkable size of $\sim 6\%$. The leptonic content can be directly evaluated in terms of the known lepton masses, yielding at one loop order:

$$\Delta\alpha_{\mathrm{lept}} = \sum_{\ell=e,\mu,\tau} \frac{\alpha}{3\pi} \left(\log\frac{M_Z^2}{m_\ell^2} - \frac{5}{3}\right) \;+\; O\left(\frac{m_\ell^2}{M_Z^2}\right)\,. \tag{7}$$

The 2-loop correction has been known already for a long time [27], and also the 3-loop contribution is now available [28], yielding altogether

$$\begin{aligned}\Delta\alpha_{\mathrm{lept}} &= 314.97687 \cdot 10^{-4} = \\ &[314.19007_{1-\mathrm{loop}} + 0.77617_{2-\mathrm{loop}} + 0.0106_{3-\mathrm{loop}}] \cdot 10^{-4}\,.\end{aligned} \tag{8}$$

For the light hadronic part, perturbative QCD is not applicable and quark masses are not available as reasonable input parameters. Instead, the 5-flavour contribution to $\hat{\Pi}^{\gamma}_{\mathrm{had}}$ can be derived from experimental data with the help of a dispersion relation

$$\Delta\alpha_{\mathrm{had}} = -\frac{\alpha}{3\pi}\, M_Z^2\, \mathrm{Re} \int_{4m_\pi^2}^{\infty} \mathrm{d}s'\, \frac{R^{\gamma}(s')}{s'(s' - M_Z^2 - i\varepsilon)} \tag{9}$$

with

$$R^{\gamma}(s) = \frac{\sigma(e^+e^- \to \gamma^* \to \mathrm{hadrons})}{\sigma(e^+e^- \to \gamma^* \to \mu^+\mu^-)}$$

as an experimental input quantity in the problematic low energy range.

Integrating by means of the trapezoidal rule (averaging data in bins) over e^+e^- data for the energy range below 40 GeV and applying perturbative QCD for the high-energy region above, the expression (9) yields the value [29,30]

$$\Delta\alpha_{\mathrm{had}} = -0.0280 \pm 0.0007\,, \tag{10}$$

which agrees with another independent analysis [31] with a different error treatment. Because of the lack of precision in the experimental data a large uncertainty is associated with the value of $\Delta\alpha_{\mathrm{had}}$, which propagates into the theoretical error of the predictions of electroweak precision observables. Including additional data from τ-decays [32] yields about the same result with a slightly improved uncertainty. Recently other attempts have been made to increase the precision of $\Delta\alpha$ [33,35]– [37] by "theory-driven" analyses of the dispersion integral (9). The common basis is the application of perturbative QCD down to the energy scale given by the τ mass for the calculation of the quantity $R^{\gamma}(s)$ outside the resonances. Those calculations were made possible by the recent availability of the quark-mass-dependent $O(\alpha_s^2)$ QCD corrections [38] for the cross section down to close to the thresholds for b and c production. [A first step in this direction was done in [39] in the massless approximation.] In order to pin down the error, two different strategies are in use: the application of the method developed in [36] for minimizing the impact of data from less reliable regions, done in [33], and the rescaling of data in the open charm region of 3.7–5 GeV from PLUTO/DASP/MARKII, for the purpose of normalization to agree with perturbative QCD, done in [35]. The results obtained for $\Delta\alpha_{\mathrm{had}}$ are very similar:

$$\begin{array}{ll} 0.02763 \pm 0.00016 & \text{ref [33]} \\ 0.02777 \pm 0.00017 & \text{ref [35]} \end{array}$$

In [37] the $\overline{MS}$ quantity $\hat{\alpha}(M_Z)$ has been derived with the help of an unsubtracted dispersion relation in the $\overline{MS}$-scheme, yielding a comparable error. The history of the determination of the hadronic vacuum polarization is visualized in Figure 1.

The basic assumption in the theory-driven approach, the validity of perturbative QCD and quark-hadron duality, is supported by the following empirical observations:

– The strong coupling constant $\alpha_s(m_\tau)$ determined from hadronic τ decays shows good agreement with $\alpha_s(M_Z)$ determined from Z-peak observables when the renormalization group evolution of α_s in perturbative QCD is imposed to run α_s from m_τ to the Z-mass scale.

– Non-perturbative contributions in $R^\gamma(s)$, parametrized in terms of condensates of quarks, gluons and of vacuum expectation values of higher-dimensional operators in the operator product expansion [40] can be probed by comparing spectral moments of $R^\gamma_{\rm exp}(s)$ with the corresponding expressions involving the theoretical R^γ. It has been shown from fitting a set of moments that the non-perturbative contributions are negligibly small [33].

– Recent preliminary measurements of R^γ at BES at 2.6 and 3.3 GeV show values slightly lower than the previous data [41,2], better in alignment with the expectations from perturbative QCD.

Although the error in the QCD-based evaluation of $\Delta\alpha_{\rm had}$ is considerably reduced, it should be kept in mind that the conservative estimate in Eq. (10) is independent of theoretical assumptions on QCD at lower energies and thus less sensitive to potential systematic effects [42].

(ii) Mixing angle renormalization and the ρ-parameter:

The ρ-parameter, originally defined as the ratio of the neutral to the charged current strength in neutrino scattering [43], is unity in the standard model at the tree level, but gets a deviation $\Delta\rho$ from 1 by radiative corrections. The dominating universal

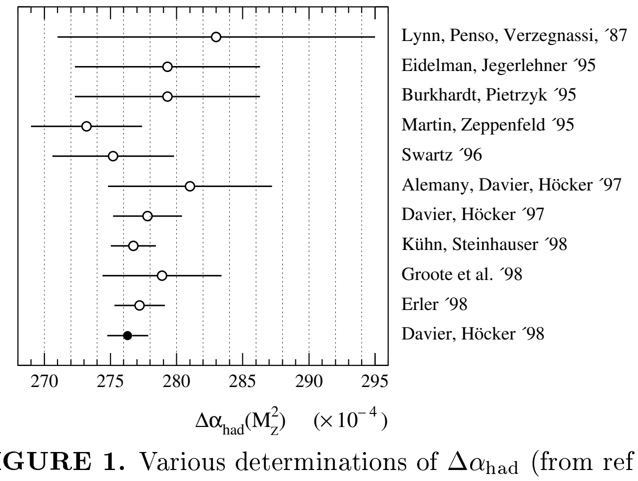

FIGURE 1. Various determinations of $\Delta\alpha_{\rm had}$ (from ref [34]).

part has its origin in the renormalization of the relation between the gauge boson masses and the electroweak mixing angle. This relation is modified in higher orders according to

$$\sin^2\theta_W = 1 - \frac{M_W^2}{M_Z^2} + \frac{M_W^2}{M_Z^2}\Delta\rho + \cdots \tag{11}$$

The main contribution to the universal ρ-parameter

$$\rho = \frac{1}{1-\Delta\rho} \tag{12}$$

is from the (t, b) doublet [44], at the present level calculated as follows:

$$\Delta\rho = 3x_t \cdot [1 + x_t\,\rho^{(2)} + \delta\rho_{\rm QCD}] \tag{13}$$

with

$$x_t = \frac{G_\mu m_t^2}{8\pi^2\sqrt{2}}\,. \tag{14}$$

The electroweak 2-loop part [45,46] is described by the function $\rho^{(2)}(M_H/m_t)$, and $\delta\rho_{\rm QCD}$ is the QCD correction to the leading $G_\mu m_t^2$ term [47,48]

$$\delta\rho_{\rm QCD} = -\frac{\alpha_s(\mu)}{\pi}\,c_1 + \left(\frac{\alpha_s(\mu)}{\pi}\right)^2 c_2(\mu) \tag{15}$$

with

$$c_1 = \frac{2}{3}\left(\frac{\pi^2}{3}+1\right) = 2.8599$$

and the 3-loop coefficient [48] $c_2(\mu)$, which amounts to

$$c_2 = -14.59 \;\; \text{for } \mu = m_t \text{ and 6 flavours}$$

with the on-shell top mass m_t. This reduces the scale dependence of ρ significantly and hence is an important entry to decrease the theoretical uncertainty of the standard model predictions for precision observables.

There is also a Higgs contribution to $\Delta\rho$, which, however, is not UV-finite by itself when derived from only the diagrams involving the physical Higgs boson. The M_H-dependence for large Higgs masses M_H is only logarithmic in 1-loop order [49]; the 2-loop contribution [50] shows a dependence $\sim M_H^2$ for large values of the Higgs mass. In the limit $\sin^2\theta_W \to 0, M_Z \to M_W$, where the $U(1)_Y$ is switched off, one finds $\Delta\rho_{\rm H} = 0$. This is the consequence of the global $SU(2)_R$ symmetry of the Higgs Lagrangian ('custodial symmetry'), which is broken by the $U(1)_Y$ group. Thus, $\Delta\rho_{\rm H}$ is a measure of the $SU(2)_R$ breaking by the weak hypercharge.

The vector boson mass correlation

The interdependence between the gauge boson masses is established through the accurately measured muon lifetime or, equivalently, the Fermi coupling constant G_μ. Originally, the μ-lifetime τ_μ has been calculated within the framework of the effective 4-point Fermi interaction. Beyond the well-known 1-loop QED corrections [51], the 2-loop QED corrections in the Fermi model have been calculated quite recently [52], yielding the expression (the error in the 2-loop term is from the hadronic uncertainty)

$$\frac{1}{\tau_\mu} = \frac{G_\mu^2 m_\mu^5}{192\pi^3}\left(1-\frac{8m_e^2}{m_\mu^2}\right)\cdot \qquad (16)$$
$$\cdot\left[1+1.810\,\frac{\alpha}{\pi}+(6.701\ \pm 0.002)\left(\frac{\alpha}{\pi}\right)^2\right].$$

This formula is the defining equation for G_μ in terms of the experimental μ-lifetime. Owing to the presence of order-dependent QED corrections, the numerical value of the Fermi constant changes after the second-order term is included. Compared with the value given in the 1998 report of the Particle Data Group [53], the latest value is now smaller by $2\cdot 10^{-10}$ GeV^{-2}, namely [52]

$$G_\mu = (1.16637 \pm 0.00001)\cdot 10^{-5}\,\mathrm{GeV}^{-2}\,, \qquad (17)$$

where also the error has been reduced by a factor of about 1/2.

In the standard model, G_μ can be calculated including quantum corrections in terms of the basic standard model parameters, thereby separating off all diagrams that correspond to the QED corrections in the Fermi model. This yields the correlation between the masses M_W, M_Z of the vector bosons, expressed in terms of α and G_μ; in 1-loop order it is given by [9]:

$$\frac{G_\mu}{\sqrt{2}} = \frac{\pi\alpha}{2s_W^2 M_W^2}[1+\Delta r(\alpha, M_W, M_Z, M_H, m_t)]\,. \qquad (18)$$

with $\quad s_W^2 = 1 - M_W^2/M_Z^2$.
The decomposition

$$\Delta r = \Delta\alpha - \frac{c_W^2}{s_W^2}\,\Delta\rho^{(1)} + (\Delta r)_{\mathrm{rem}} \qquad (19)$$

separates the leading fermionic contributions $\Delta\alpha$ and $\Delta\rho$(1-loop). All other terms are collected in the remainder part $(\Delta r)_{\mathrm{rem}}$, the typical size of which is of order ~ 0.01.

The presence of large terms in Δr requires the consideration of effects higher than 1-loop. The modification of Eq. (18) according to

$$1+\Delta r \;\to\; \frac{1}{(1-\Delta\alpha)\cdot(1+\frac{c_W^2}{s_W^2}\Delta\rho) \;-\; (\Delta r)_{\text{rem}}}$$
$$\equiv \; \frac{1}{1-\Delta r} \tag{20}$$

accommodates the following higher-order terms (Δr in the denominator is an effective correction including higher orders):

(i) the leading log resummation [54] of $\Delta\alpha$: $1+\Delta\alpha \;\to\; (1-\Delta\alpha)^{-1}$;

(ii) the resummation of the leading m_t^2 contribution [55] in terms of $\Delta\rho$ in Eq. (13). Beyond the QCD higher-order contributions through the ρ-parameter, the complete $O(\alpha\alpha_s)$ corrections to the self energies are available [56,57]. All these higher-order terms contribute with the same positive sign to Δr. Non-leading QCD corrections to Δr of the type

$$\Delta r_{(bt)} = 3x_t \left(\frac{\alpha_s}{\pi}\right)^2 \left(a_1 \frac{M_Z^2}{m_t^2} + a_2 \frac{M_Z^4}{m_t^4}\right)$$

are also available [58].

(iii) With the quantity $(\Delta r)_{\text{rem}}$ in the denominator, non-leading higher-order terms containing mass singularities of the type $\alpha^2 \log(M_Z/m_f)$ from light fermions are incorporated [59].

(iv) The subleading $G_\mu^2 m_t^2 M_Z^2$ contribution of the electroweak 2-loop order [60] in an expansion in terms of the top mass. This subleading term turned out to be sizeable, about as large as the formally leading term of $O(m_t^4)$ via the ρ-parameter. In view of the present and future experimental accuracy it constitutes a non-negligible shift in the W mass.

Meanwhile exact results have been derived for the Higgs-dependence of the fermionic 2-loop corrections in Δr [61], and comparisons were performed with those obtained via the top mass expansion [62]. Differences in the values of M_W of several MeV (up to 8 MeV) are observed when M_H is varied over the range from 65 GeV to 1 TeV.

Figure 2 shows the Higgs-mass dependence of the two-loop corrections to Δr associated with the t/b doublet, with $\Delta\alpha$, and with the light fermion terms not in $\Delta\alpha$, together with the leading m_t^4-term, which constitutes a very poor approximation.

Pure fermion-loop contributions (n fermion loops at n-loop order) have also been investigated [62,63]. In the on-shell scheme, explicit results have been worked out up to 4-loop order, which allows an investigation of the validity of the resummation (20) for the non-leading 2-loop and higher-order terms. It was found that numerically the resummation (20) works remarkably well, within 2 MeV in M_W.

Observables at the Z resonance

Measurements of the Z line shape in $e^+e^- \to f\bar{f}$ yield the parameters M_Z, Γ_Z, and the partial widths Γ_f or the peak cross section

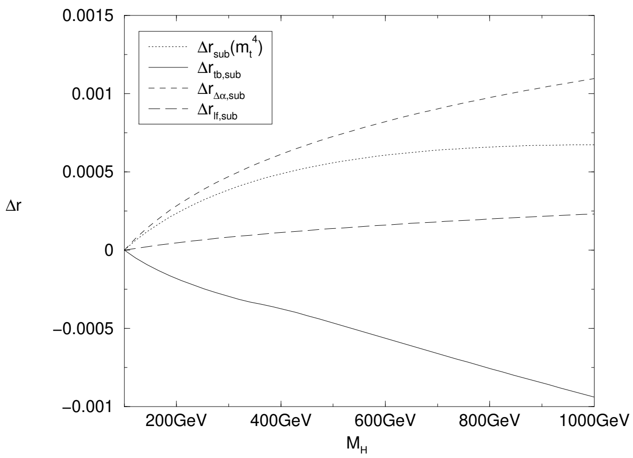

FIGURE 2. Higgs mass dependence of fermionic contributions to Δr at the two-loop level (from [62]). The different curves show the various contributions: light fermions via $\Delta\alpha$ ($\Delta r_{\Delta\alpha}$), residual light-fermion contribution not in $\Delta\alpha$ ($\Delta r_{\rm lf}$), the contribution from the (tb) doublet ($\Delta r_{\rm tb}$), and the approximation of the (tb) two-loop contribution by the term proportional to m_t^4. Displayed in each case is the difference $\Delta r(M_H) - \Delta r(100\text{ GeV})$.

$$\sigma_0^f = \frac{12\pi}{M_Z^2} \cdot \frac{\Gamma_e \Gamma_f}{\Gamma_Z^2}\,. \tag{21}$$

Angular distributions and polarization measurements of the final fermions yield forward–backward and polarization asymmetries. Whereas M_Z is used as a precise input parameter, together with α and G_μ, the width, partial widths and asymmetries allow comparisons with the predictions of the standard model. The predictions for the partial widths as well as for the asymmetries can conveniently be calculated in terms of effective neutral current coupling constants for the various fermions.

Effective Z boson couplings: The effective couplings follow from the set of 1-loop diagrams without virtual photons, the non-QED or weak corrections. These weak corrections can conveniently be written in terms of fermion-dependent overall normalizations ρ_f and effective mixing angles s_f^2 in the NC vertices (see e.g. [64]):

$$\begin{aligned} J_\nu^{\rm NC} &= \left(\sqrt{2}G_\mu M_Z^2\right)^{1/2} \left(g_V^f\,\gamma_\nu - g_A^f\,\gamma_\nu\gamma_5\right) \\ &= \left(\sqrt{2}G_\mu M_Z^2 \rho_f\right)^{1/2} \left((I_3^f - 2Q_f s_f^2)\gamma_\nu - I_3^f \gamma_\nu\gamma_5\right). \end{aligned} \tag{22}$$

ρ_f and s_f^2 contain universal parts, e.g. from the ρ-parameter via

$$\rho_f = \frac{1}{1-\Delta\rho} + \cdots, \quad s_f^2 = s_W^2 + c_W^2\,\Delta\rho + \cdots \tag{23}$$

with $\Delta\rho$ from Eq. (13) and non-universal parts that explicitly depend on the type of the external fermions.

The subleading 2-loop corrections $\sim G_\mu^2 m_t^2 M_Z^2$ for the leptonic mixing angle [60] s_ℓ^2 have also be obtained in the meantime, as well as for ρ_ℓ [65].

Meanwhile exact results have been derived for the Higgs-dependence of the fermionic 2-loop corrections in s_ℓ^2 [62,63], and comparisons were performed with those obtained via the top mass expansion [62]. Differences in the values of s_ℓ^2 can amount to $0.8 \cdot 10^{-4}$ when M_H is varied over the range from 100 GeV to 1 TeV.

For the b quark coupling to the Z boson, not only the universal contribution through the ρ-parameter but also the non-universal parts have a strong dependence on m_t, resulting from virtual top quarks in the vertex corrections. The difference between the d and b couplings can be parametrized in the following way

$$\rho_b = \rho_d (1+\tau)^2, \quad s_b^2 = s_d^2 (1+\tau)^{-1}, \tag{24}$$

with the quantity

$$\tau = \Delta\tau^{(1)} + \Delta\tau^{(2)}$$

calculated perturbatively, including the complete 1-loop order term [66] with x_t from Eq. (14):

$$\Delta\tau^{(1)} = -2x_t - \frac{G_\mu M_Z^2}{6\pi^2\sqrt{2}}(c_W^2+1)\log\frac{m_t}{M_W} + \cdots, \tag{25}$$

and the leading electroweak 2-loop contribution of $O(G_\mu^2 m_t^4)$ [46,67]

$$\Delta\tau^{(2)} = -2\, x_t^2\, \tau^{(2)}, \tag{26}$$

where $\tau^{(2)}$ is a function of M_H/m_t with $\tau^{(2)} = 9 - \pi^2/3$ for small M_H.

Asymmetries and mixing angles: The effective mixing angles are of particular interest, since they determine the on-resonance asymmetries via the combinations

$$A_f = \frac{2 g_V^f g_A^f}{(g_V^f)^2 + (g_A^f)^2}, \tag{27}$$

namely

$$A_{\rm FB} = \frac{3}{4} A_e A_f, \quad A_\tau^{\rm pol} = A_\tau, \quad A_{\rm LR} = A_e \,. \tag{28}$$

Measurements of the asymmetries hence are measurements of the ratios

$$g_V^f/g_A^f = 1 - 2Q_f s_f^2 \tag{29}$$

or the effective mixing angles, respectively.

Z width and partial widths: The total Z width Γ_Z can be calculated essentially as the sum over the fermionic partial decay widths. Expressed in terms of the effective coupling constants, they read up to second order in the fermion masses:

$$\Gamma_f = \Gamma_0 \left[(g_V^f)^2 + (g_A^f)^2 \left(1 - \frac{6m_f^2}{M_Z^2} \right) \right] \cdot \left(1 + Q_f^2 \frac{3\alpha}{4\pi} \right) + \Delta\Gamma_{\rm QCD}^f$$

with

$$\Gamma_0 \; = \; N_C^f \, \frac{\sqrt{2} G_\mu M_Z^3}{12\pi}, \quad N_C^f = 1 \text{ (leptons)}, \quad = 3 \text{ (quarks)}.$$

The QCD correction for the light quarks with $m_q \simeq 0$ is given by

$$\Delta\Gamma_{\rm QCD}^f \; = \; \Gamma_0 \left((g_V^f)^2 + (g_A^f)^2 \right) \cdot K_{\rm QCD} \tag{30}$$

with [68]

$$K_{\rm QCD} = \frac{\alpha_s}{\pi} + 1.41 \left(\frac{\alpha_s}{\pi} \right)^2 - 12.8 \left(\frac{\alpha_s}{\pi} \right)^3 - \frac{Q_f^2}{4} \frac{\alpha \alpha_s}{\pi^2} \, .$$

For b quarks the QCD corrections are different, because of finite b mass terms and to top-quark-dependent 2-loop diagrams for the axial part:

$$\Delta\Gamma_{\rm QCD}^b = \Delta\Gamma_{\rm QCD}^d \, + \, \Gamma_0 \left[(g_V^b)^2 \, R_V \, + \, (g_A^b)^2 \, R_A \right] . \tag{31}$$

The coefficients in the perturbative expansions

$$R_V = c_1^V \frac{\alpha_s}{\pi} + c_2^V \left(\frac{\alpha_s}{\pi} \right)^2 + c_3^V \left(\frac{\alpha_s}{\pi} \right)^3 + \cdots,$$
$$R_A = c_1^A \frac{\alpha_s}{\pi} + c_2^A \left(\frac{\alpha_s}{\pi} \right)^2 + \cdots$$

depending on m_b and m_t, are calculated up to third order in α_s, except for the m_b-dependent singlet terms, which are known to $O(\alpha_s^2)$ [69,70]. For a review of the QCD corrections to the Z width, see [71].

The partial decay rate into b-quarks, in particular the ratio $R_b = \Gamma_b/\Gamma_{\rm had}$, is an observable of special sensitivity to the top quark mass. Therefore, beyond the pure QCD corrections, also the 2-loop contributions of the mixed QCD–electroweak type, are important. The QCD corrections were first derived for the leading term of $O(\alpha_s G_\mu m_t^2)$ [72] and were subsequently completed by the $O(\alpha_s)$ correction to the $\log m_t/M_W$ term [73] and the residual terms of $O(\alpha\alpha_s)$ [74].

In the same spirit, also the complete 2-loop $O(\alpha\alpha_s)$ to the partial widths into the light quarks have been obtained, beyond those that are already contained in the factorized expression (30) with the electroweak 1-loop couplings [75]. These "non-factorizable" corrections yield an extra negative contribution of $-0.55(3)$ MeV to the total hadronic Z width (converted into a shift of the strong coupling constant, they correspond to $\delta\alpha_s = 0.001$). In summary, the 2-loop corrections of $O(\alpha\alpha_s)$ to the electroweak precision observables are by now completely under control.

Radiation of secondary fermions through photons from the primary final state fermions can yield another sizeable contribution to the partial Z widths; however, this is compensated by the corresponding virtual contribution through the dressed photon propagator in the final-state vertex correction for sufficiently inclusive final states, i.e. for loose cuts to the invariant mass of the secondary fermions [76].

Accuracy of the standard model predictions

For a discussion of the theoretical reliability of the standard model predictions, one has to consider the various sources contributing to their uncertainties:

Parametric uncertainties result from the limited precision in the experimental values of the input parameters, essentially $\alpha_s = 0.119 \pm 0.002$ [53], $m_t = 173.8 \pm 5.0$ GeV [5], $m_b = 4.7 \pm 0.2$ GeV, and the hadronic vacuum polarization as discussed in section 2.1. The conservative estimate of the error in Eq. (10) leads to $\delta M_W = 13$ MeV in the W-mass prediction, and $\delta \sin^2\theta = 0.00023$ common to all of the mixing angles.

The uncertainties from the QCD contributions can essentially be traced back to those in the top quark loops in the vector boson self-energies. The knowledge of the $O(\alpha_s^2)$ corrections to the ρ-parameter and Δr yields a significant reduction; they are small, although not negligible (e.g. $\sim 3 \cdot 10^{-5}$ in s_ℓ^2).

The size of unknown higher-order contributions can be estimated by different treatments of non-leading terms of higher order in the implementation of radiative corrections in electroweak observables ('options') and by investigations of the scheme dependence. Explicit comparisons between the results of 5 different computer codes based on on-shell and $\overline{MS}$ calculations for the Z-resonance observables are documented in the "Electroweak Working Group Report" [64] in ref [26]. The inclusion of the non-leading 2-loop corrections $\sim G_\mu^2 m_t^2 M_Z^2$ reduce the uncertainty in M_W below 10 MeV and in s_ℓ^2 below 10^{-4}, typically to $\pm 4 \cdot 10^{-5}$ [82].

PRECISION DATA AND THE STANDARD MODEL

We now confront the standard model predictions for the discussed set of precision observables with the most recent sample of experimental data [1,2]. In table 1 the standard model predictions for Z-pole observables and the W mass are put together for the best fit input data set, given in (33). The experimental results on the Z observables are from LEP and the SLC, the W mass is from combined LEP and $p\bar{p}$ data. The leptonic mixing angle determined via $A_{\rm LR}$ by the SLD experiment [77] and the s_ℓ^2 average from LEP:

$$s_e^2(A_{\rm LR}) = 0.23109 \pm 0.00029, \quad s_\ell^2(\rm LEP) = 0.23189 \pm 0.00024$$

TABLE 1. Precision observables: experimental results from combined LEP and SLD data for Z observables and combined $p\bar{p}$ and LEP data for M_W, together with the standard model predictions for the best fit, Eq. (33).

Observable	Exp.	SM best fit
M_Z (GeV)	91.1867 ± 0.0019	91.1865
Γ_Z (GeV)	2.4939 ± 0.0024	2.4956
σ_0^{had} (nb)	41.491 ± 0.058	41.476
R_{had}	20.765 ± 0.026	20.745
R_b	0.21656 ± 0.00074	0.2159
R_c	0.1732 ± 0.0048	0.1722
$A_{\rm FB}^{\ell}$	0.01683 ± 0.00096	0.0162
$A_{\rm FB}^{b}$	0.0990 ± 0.0021	0.1029
$A_{\rm FB}^{c}$	0.0709 ± 0.0044	0.0735
A_b	0.867 ± 0.035	0.9347
A_c	0.647 ± 0.040	0.6678
ρ_ℓ	1.0041 ± 0.0012	1.0051
s_ℓ^2	0.23157 ± 0.00018	0.23155
M_W (GeV)	80.39 ± 0.06	80.372

have come closer to each other in their central value; owing to their smaller errors, however, they still differ by 2.8 standard deviations.

Table 1 contains the combined LEP/SLD value. ρ_ℓ and s_ℓ^2 are the leptonic neutral current couplings in Eq. (22), derived from partial widths and asymmetries under the assumption of lepton universality.

Note that the experimental value for ρ_ℓ points at the presence of genuine electroweak corrections by 3.5 standard deviations. In s_ℓ^2 the presence of purely bosonic radiative corrections is clearly established when the experimental result is compared with a theoretical value containing only the fermion loop corrections, an observation that has been persisting already for several years [78]. The deviation from the standard model prediction in the quantity R_b has been reduced below one standard deviation by now. Other small deviations are observed in the asymmetries: the purely leptonic $A_{\rm FB}$ is slightly higher than the standard model predictions, and $A_{\rm FB}$ for b quarks is lower. Whereas the leptonic $A_{\rm FB}$ favours a very light Higgs boson, the b quark asymmetry needs a heavy Higgs.

The effective mixing angle is an observable most sensitive to the mass M_H of the Higgs boson. Since a light Higgs boson corresponds to a low value of s_ℓ^2, the strongest upper bound on M_H is from $A_{\rm LR}$ at the SLC [77]. The inclusion of the two-loop electroweak corrections $\sim m_t^2$ from [60] yields a sizeable positive contribution to s_ℓ^2, see Figure 3. The inclusion of this term hence strengthens the upper bound on M_H.

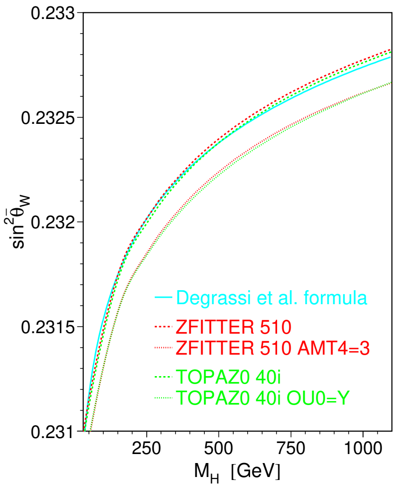

FIGURE 3. Higgs mass dependence of s_ℓ^2 with and without the electroweak 2-loop term $\sim m_t^2$, comparison of ZFITTER and TOPAZ0 codes. The lower sample of curves is without, the upper sample with the 2-loop term (figure prepared by C. Pauss).

The W mass prediction in table 1 is obtained from Eq. (18) (including the higher-order terms) from M_Z, G_μ, α and M_H, m_t. The present experimental value for the W mass from the combined LEP 2, UA2, CDF and D0 results is in best agreement with the standard model prediction.

The quantity s_W^2 resp. the ratio M_W/M_Z can indirectly be measured in deep-inelastic neutrino–nucleon scattering. The average from the experiments CCFR, CDHS and CHARM with the recent NUTEV result [79]

$$s_W^2 = 1 - M_W^2/M_Z^2 = 0.2255 \pm 0.0021 \tag{32}$$

for $m_t = 175$ GeV and $M_H = 150$ GeV corresponds to $M_W = 80.25 \pm 0.11$ GeV and is hence consistent with the direct vector boson mass measurements and with the standard theory.

Standard model global fits: The FORTRAN codes ZFITTER [80] and TOPAZ0 [81] have been updated by incorporating all the recent precision calculation results that were discussed in the previous section. Comparisons have shown good agreement between the predictions from the two independent programs [82]. Global fits of the standard model parameters to the electroweak precision data done by the Electroweak Working Group [1] are based on these recent versions. Including m_t and M_W from the direct measurements in the experimental data set, together with s_W^2 from neutrino scattering, the standard model parameters for the best fit result are:

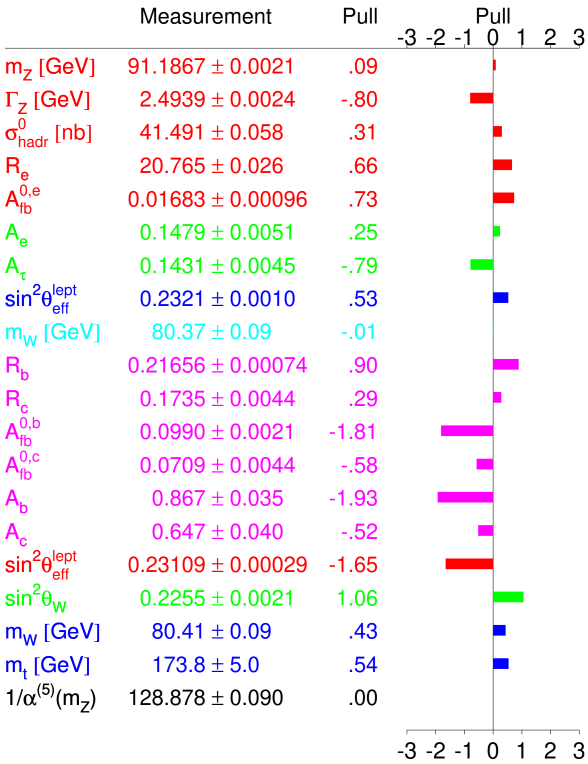

FIGURE 4. Experimental results and pulls from a standard model fit (from ref [1,2]). pull = obs(exp)-obs(SM)/(exp.error).

$$
\begin{aligned}
m_t &= 171.1 \pm 4.9\,\text{GeV} \\
M_H &= 76^{+85}_{-47}\,\text{GeV} \\
\alpha_s &= 0.119 \pm 0.003\,.
\end{aligned}
\tag{33}
$$

The upper limit to the Higgs mass at the 95% C.L. is $M_H < 262$ GeV, where the theoretical uncertainty is included. Thereby the hadronic vacuum polarization in Eq. (10) has been used (solid line in Figure 5). With the theory-driven result on $\Delta\alpha_{\text{had}}$ of ref [33] one obtains [1] $M_H = 92^{+64}_{-41}$ (dashed line). The 1σ upper bound on M_H is influenced only marginally. The reason is that simultaneously with the error reduction the central value of M_H is shifted upwards (see Figure 5). Another recent analysis [83] (for earlier studies see [84,85]) based on the data set of summer 1998 yields a Higgs mass $M_H = 107^{+67}_{-45}$ GeV. About one half of the difference with (33) can be ascribed to the use of $\alpha(M_Z)$ of ref [37], which is very close to the value in ref [33,35]; the residual shift might be interpreted as due to different renormalization schemes and different treatments of α_s.

With an overall χ^2/d.o.f. = 15/15 the quality of the fit is remarkably high. As can be seen from Figure 4, the deviation of the individual quantities from the standard model best-fit values are below 2 standard deviations.

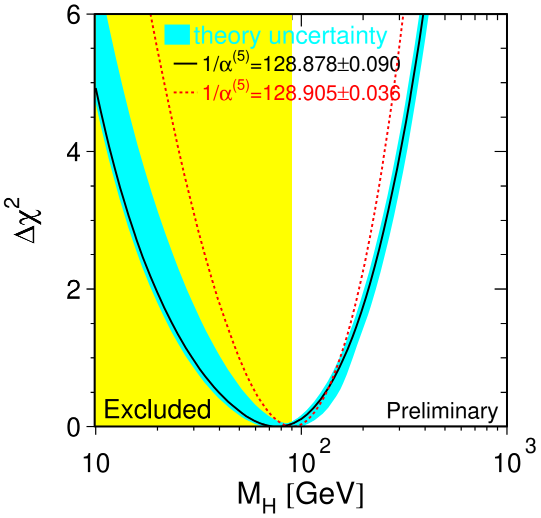

FIGURE 5. Higgs mass dependence of χ^2 in the global fit to precision data (from ref [1,2]). The shaded band displays the error from the theoretical uncertainties obtained from various options in the codes ZFITTER and TOPAZ0.

Compared with the results from 1997, the central value for the Higgs mass has moved to lower values and the error has been decreased. The Higgs mass bounds follow from the χ^2 distribution shown in Figure 5. The shift in the central value illustrates the effect of the inclusion of the electroweak two-loop contribution by Degrassi et al. [60], which was not implemented in the codes for the earlier analyses. Since it increases the prediction for s_ℓ^2 (Figure 3) for a given Higgs mass, the allowed values of M_H are shifted accordingly downwards.

The second observation is the decrease of the error, which besides the experimental improvements results from the reduction of the theoretical uncertainties of pure electroweak origin. The shaded band around the solid line in Figure 5 is the influence of the various 'options' (see section 2.4) in the codes ZFITTER and TOPAZ0 after the implementation of the 2-loop electroweak terms $\sim m_t^2$. It is thus the direct continuation of the error estimate done in the previous study [64]. Compared with the width of the uncertainty band in 1997 the shrinking is evident.

On the other hand, the remaining theoretical uncertainty associated with the Higgs mass bounds should be taken very seriously. The effect of the inclusion of the next-to-leading term in the m_t-expansion of the electroweak 2-loop corrections in the precision observables has shown to be sizeable, at the upper margin of the estimate given in [64]. It is thus not guaranteed that the subsequent subleading terms in the m_t-expansion are indeed smaller in size. Also the variation of the M_H-dependence at different stages of the calculation, as discussed in the previous subsections, indicate the necessity of more complete results at two-loop order. Having in mind also the variation of the Higgs mass bounds under the fluctuations of the experimental data [2], the limits for M_H derived from the analysis of electroweak data in the frame of the standard model still carry a noticeable uncertainty. Nevertheless, as a central message, it can be concluded that the indirect determination of the Higgs mass range has shown that the Higgs is light, with its mass well below the non-perturbative regime.

THE STANDARD HIGGS SECTOR

The minimal model with a single scalar doublet is the simplest way to implement the electroweak symmetry breaking. The experimental result that the ρ-parameter is very close to unity is a natural feature of models with doublets and singlets. In the standard model, the mass M_H of the Higgs boson appears as the only additional parameter beyond the vector boson and fermion masses. M_H cannot be predicted but has to be taken from experiment. The present lower limit (95% C.L.) from the search at LEP [86] is 89 GeV. Indirect determinations of M_H from precision data have already been discussed in section 3. The indirect mass bounds react sensitively to small changes in the input data, which is a consequence of the logarithmic dependence of electroweak precision observables. As a general feature, it appears that the data prefer a light Higgs boson.

There are also theoretical constraints on the Higgs mass from vacuum stability and absence of a Landau pole [87–89], and from lattice calculations [90]. Explicit perturbative calculations of the decay width for $H \to W^+W^-, ZZ$ in the large-M_H limit in 2-loop order [92] have shown that the 2-loop contribution exceeds the 1-loop term in size (same sign) for $M_H > 930$ GeV (Figure 6). This result is confirmed by the calculation of the next-to-leading order correction in the $1/N$ expansion, where the Higgs sector is treated as an $O(N)$ symmetric σ-model [93]. A similar increase of the 2-loop perturbative contribution with M_H is observed for the fermionic decay [94] $H \to f\bar{f}$, but with opposite sign leading to a cancellation of the one-loop correction for $M_H \simeq 1100$ GeV (Figure 6). The requirement of applicability of perturbation theory therefore puts a stringent upper limit on the Higgs mass. The indirect Higgs mass bounds obtained from the precision analysis show, however, that the Higgs boson is well below the mass range where the Higgs sector becomes non-perturbative. The lattice result [91] for the bosonic Higgs decay in Figure 6 for $M_H = 727$ GeV is not far from the perturbative 2-loop result. The difference may at least partially be interpreted as missing higher-order terms.

The behaviour of the quartic Higgs self-coupling λ, as a function of a rising energy scale μ, follows from the renormalization group equation with the β-function dominated by λ and the top quark Yukawa coupling g_t contributions:

$$\beta_\lambda = 24\,\lambda^2 + 12\,\lambda\,g_t^2 - 6\,g_t^4 + \cdots \tag{34}$$

In order to avoid unphysical negative quartic couplings from the negative top quark contribution, a lower bound on the Higgs mass is derived. The requirement that the Higgs coupling remains finite and positive up to a scale Λ yields constraints

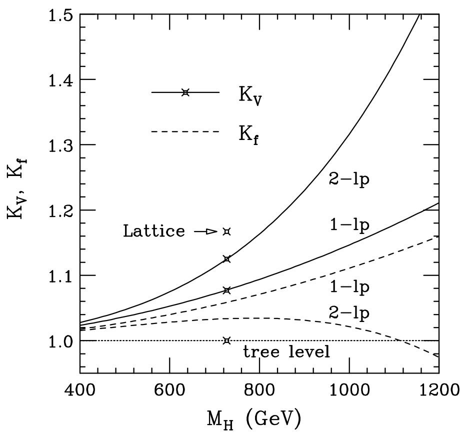

FIGURE 6. Correction factors for the Higgs decay widths $H \to VV$ $(V = W, Z)$ and $H \to f\bar{f}$ in 1- and 2-loop order (from ref [95])

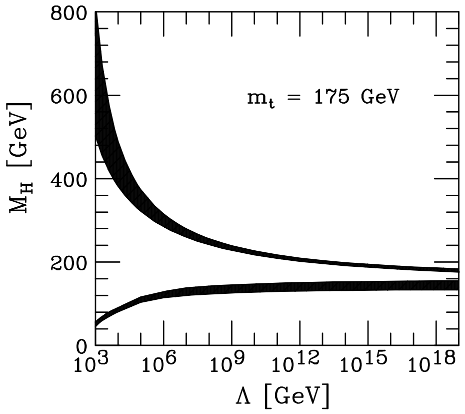

FIGURE 7. Theoretical limits on the Higgs boson mass from the absence of a Landau pole and from vacuum stability (from ref [89])

on the Higgs mass M_H, which have been evaluated at the 2-loop level [88,89]. These bounds on M_H are shown in Figure 7 as a function of the cut-off scale Λ up to which the standard Higgs sector can be extrapolated, for $m_t = 175$ GeV and $\alpha_s(M_Z) = 0.118$. The allowed region is the area between the lower and the upper curves. The bands indicate the theoretical uncertainties associated with the solution of the renormalization group equations [89]. It is interesting to note that the indirect determination of the Higgs mass range from electroweak precision data via radiative corrections is compatible with a value of M_H where Λ can extend up to the Planck scale.

PRECISION TESTS OF THE MSSM

Among the extensions of the standard model, the MSSM is the theoretically favoured scenario as the most predictive framework beyond the standard model. A

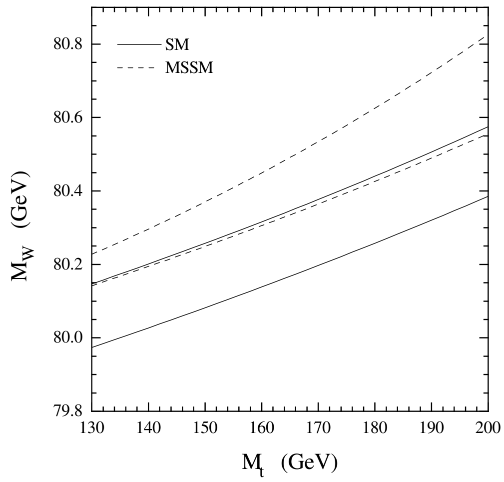

FIGURE 8. The W mass range in the standard model (—–) and the MSSM (- - -). Bounds are from the non-observation of Higgs bosons and SUSY particles at LEP2.

definite prediction of the MSSM is the existence of a light Higgs boson with mass below $\sim$ 135 GeV [107–109,112]. The detection of a light Higgs boson at LEP could be a significant hint for supersymmetry.

The structure of the MSSM as a renormalizable quantum field theory allows a similarly complete calculation of the electroweak precision observables as in the standard model in terms of one Higgs mass (usually taken as the CP-odd 'pseudoscalar' mass M_A) and $\tan\beta = v_2/v_1$, together with the set of SUSY soft-breaking parameters fixing the chargino/neutralino and scalar fermion sectors. It has been known for quite some time [96] that light non-standard Higgs bosons as well as light stop and charginos predict larger values for the ratio R_b [97,99,105]. Complete 1-loop calculations are available for Δr and for the Z boson observables [98,99,105].

So far, the direct search of SUSY particles at colliders has not been successful, and under some assumptions one can only set lower bounds on their masses. An alternative way to probe SUSY is to search for the virtual effects of the additional particles. One can use the high-precision measurements of electroweak observables to search for the quantum effects of the SUSY particles. In the MSSM one finds two types of potentially large effects: The first possibility is that charginos and scalar top quarks are light enough to affect the decay width of the Z boson into b–quarks; however, for masses beyond the LEP2 or Tevatron reach, these effects become too small to be observable. The second possibility is the contribution of the top and bottom squark loops to the electroweak gauge–boson self–energies: if there is a large splitting between the masses of $\tilde{b}_L$ and $\tilde{t}_L$, the contribution will grow with the mass of the heaviest scalar quark and can be sizable. This contribution enters the electroweak observables via the ρ parameter, which influences the normalization of the NC Z couplings, the effective electroweak mixing angle at the Z–boson resonance and the $W - Z$ mass correlation. Recently the 2-loop α_s corrections have been computed [100], which can amount to 30% of the 1-loop $\Delta\rho_{\tilde{b}\tilde{t}}$.

Figure 8 displays the range of predictions for M_W in the minimal model and in the MSSM. It is thereby assumed that no direct discovery has been made at LEP 2. As can be seen, precise determinations of M_W and m_t can become decisive for the separation between the models.

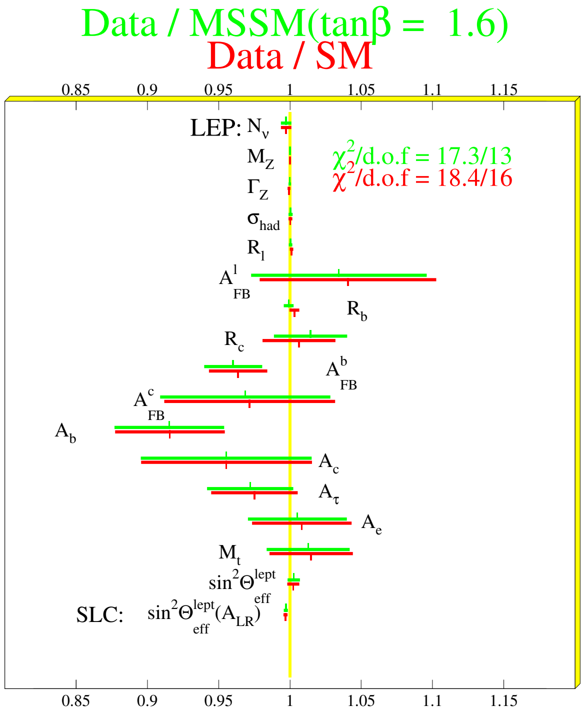

FIGURE 9. Best fits in the SM and in the MSSM, normalized to the data. Error bars are those from data. (Updated from ref [85] by U. Schwickerath).

As the standard model, the MSSM yields a good description of the precision data. A global fit [85] to all electroweak precision data, including the top mass measurement, shows that the χ^2 of the fit is slightly better than in the standard model; but, owing to the larger numbers of parameters, the probability is about the same as for the standard model (Figure 9).

The virtual presence of SUSY particles in the precision observables can be exploited also in the other way of constraining the allowed range of the MSSM parameters. Since the quality of the standard model description can be achieved only for those parameter sets where the standard model with a light Higgs boson is approximated, deviations from this scenario result in a rapid decrease of the fit quality. An analysis of the precision data in this spirit can be found in ref [101].

THE MASS OF THE LIGHTEST MSSM HIGGS BOSON

The search for the lightest Higgs boson provides a direct and very stringent test of SUSY. A precise prediction for the mass of the lightest Higgs boson in terms of the relevant SUSY parameters hence is crucial in order to determine the discovery and exclusion potential of LEP2 and the upgraded Tevatron and also for physics at the LHC, where a high-precision measurement of the mass of this particle might be possible.

In the MSSM, the mass m_h of the lightest Higgs boson is restricted at the tree level to be smaller than the Z-boson mass. This bound, however, is strongly affected by the inclusion of radiative corrections. The dominant one-loop corrections arise form the top and scalar-top sector via terms of the form $G_F m_t^4 \ln(m_{\tilde{t}_1} m_{\tilde{t}_2}/m_t^2)$ [102]. They increase the predicted values of m_h and yield an upper bound of about 150 GeV. These results have been improved by performing a complete one-loop calculation in the on-shell scheme, which takes into account the contributions of all sectors of the MSSM [103–105]. Beyond one-loop order renormalization group (RG) methods have been applied in order to obtain leading logarithmic higher-order contributions [106–109], and a diagrammatic calculation of the dominant two-loop contributions in the limiting case of vanishing $\tilde{t}$-mixing and infinitely large M_A and $\tan\beta$ has been carried out [110].

Recently a Feynman-diagrammatic calculation of the leading two-loop corrections of $\mathcal{O}(\alpha\alpha_s)$ to the masses of the neutral $\mathcal{CP}$-even Higgs bosons has been performed [111]. They have been combined with the complete one-loop diagrammatic calculation [112] to obtain in this way the currently most precise prediction for m_h within the Feynman-diagrammatic approach for arbitrary values of the parameters of the Higgs and scalar top sector of the MSSM. Further refinements concerning the leading two-loop Yukawa corrections of $\mathcal{O}(G_F^2 m_t^6)$ [107] and of leading QCD corrections beyond two-loop order are also included. The results will be discussed in this section.

In the MSSM two Higgs doublets are needed, decomposed as follows:

$$\begin{aligned} H_1 &= \begin{pmatrix} H_1^1 \\ H_1^2 \end{pmatrix} = \begin{pmatrix} v_1 + (\phi_1^0 + i\chi_1^0)/\sqrt{2} \\ \phi_1^- \end{pmatrix}, \\ H_2 &= \begin{pmatrix} H_2^1 \\ H_2^2 \end{pmatrix} = \begin{pmatrix} \phi_2^+ \\ v_2 + (\phi_2^0 + i\chi_2^0)/\sqrt{2} \end{pmatrix}. \end{aligned} \tag{35}$$

The Higgs sector can be described with the help of two independent parameters (besides the gauge couplings g, g'), usually chosen as $\tan\beta = v_2/v_1$ and the mass M_A of the $\mathcal{CP}$-odd A boson. The $\mathcal{CP}$-even neutral mass eigenstates h^0, H^0 are obtained from $\phi_{1,2}^0$ by a rotation yielding the tree-level masses $m_{h,H,\mathrm{tree}}$.

In the Feynman-diagrammatic approach the one-loop corrected Higgs masses are derived by finding the poles of the $h-H$-propagator matrix whose inverse is given by

$$\begin{pmatrix} q^2 - m^2_{H,\mathrm{tree}} + \hat{\Sigma}_H(q^2) & \hat{\Sigma}_{hH}(q^2) \\ \hat{\Sigma}_{hH}(q^2) & q^2 - m^2_{h,\mathrm{tree}} + \hat{\Sigma}_h(q^2) \end{pmatrix}, \tag{36}$$

where the $\hat{\Sigma}$ denote the full one-loop contributions to the renormalized Higgs-boson self-energies, which are taken from the complete one-loop on-shell calculation of [104]. The agreement with the result obtained in [103] is better than 1 GeV for almost the whole MSSM parameter space.

As mentioned above the dominant contribution arises from the $t-\tilde{t}$-sector. The current eigenstates of the scalar quarks, $\tilde{q}_L$ and $\tilde{q}_R$, mix to give the mass eigenstates $\tilde{q}_1$ and $\tilde{q}_2$. The non-diagonal entry in the scalar quark mass matrix is proportional to the mass of the quark and reads for the $\tilde{t}$-mass matrix

$$m_t M_t^{LR} = m_t(A_t - \mu\cot\beta\ ). \tag{37}$$

Due to the large value of m_t mixing effects have to be taken into account. Diagonalizing the $\tilde{t}$-mass matrix one obtains the eigenvalues $m_{\tilde{t}_1}$ and $m_{\tilde{t}_2}$ and the $\tilde{t}$ mixing angle $\theta_{\tilde{t}}$.

The leading two-loop corrections have been obtained in [111] by calculating the $\mathcal{O}(\alpha\alpha_s)$ contribution of the $t-\tilde{t}$-sector to the renormalized Higgs-boson self-energies at zero external momentum from the Yukawa part of the theory. At the two-loop level the matrix (36) consists of the renormalized Higgs-boson self-energies

$$\hat{\Sigma}_s(q^2) = \hat{\Sigma}_s^{(1)}(q^2) + \hat{\Sigma}_s^{(2)}(0), \quad s = h, H, hH, \tag{38}$$

where the momentum dependence is neglected only in the two-loop contribution. The Higgs-boson masses at the two-loop level are obtained by determining the poles of the matrix Δ_{Higgs} in Eq. (36).

Two further steps of refinement have been implemented into the prediction for m_h, which are shown separately in the plots below. The leading two-loop Yukawa correction of $\mathcal{O}(G_F^2 m_t^6)$ is taken over from the result obtained by renormalization group methods [107]. The second step of refinement concerns leading QCD corrections beyond two-loop order, taken into account by using the $\overline{MS}$ top mass, $\overline{m}_t = \overline{m}_t(m_t) \approx 166.5$ GeV, for the two-loop contributions instead of the pole mass, $m_t = 175$ GeV. In the $\tilde{t}$ mass matrix, however, the pole mass is used as an input parameter. Only when performing the comparison with the RG results, m_t is replaced by $\overline{m}_t$ in the $\tilde{t}$ mass matrix for the two-loop result, since in the RG results the running masses appear everywhere. This three-loop effect gives rise to a shift up to 1.5 GeV in the prediction for m_h.

For the quantitative illustration, two representative values for $\tan\beta$ (favored by SUSY-GUT scenarios) are chosen: $\tan\beta\ = 1.6$ for the $SU(5)$ scenario and $\tan\beta\ = 40$ for the $SO(10)$ scenario; other parameters are $\alpha_s(m_t) = 0.1095$, and $m_t = 175$ GeV. For the figures below, furthermore $M = 400$ GeV ($M \equiv M_2$ is the soft SUSY breaking gaugino mass parameter), $M_A = 500$ GeV, and $m_{\tilde{g}} = 500$ GeV as typical values. The scalar top masses and the mixing angle are derived from

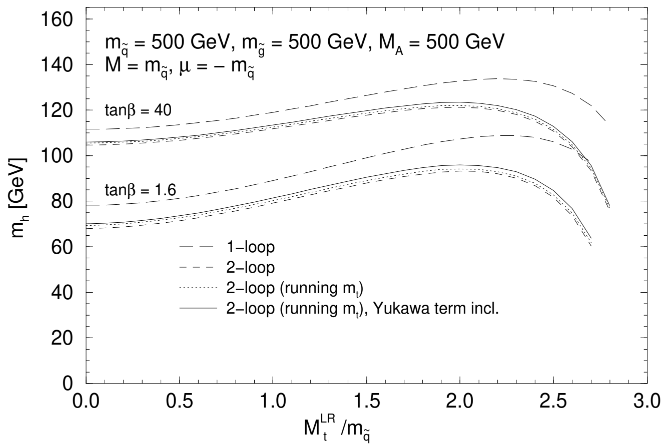

FIGURE 10. One- and two-loop results for m_h as a function of $M_t^{LR}/m_{\tilde{q}}$ for two values of $\tan\beta$.

the parameters $M_{\tilde{t}_L}$, $M_{\tilde{t}_R}$ and M_t^{LR} of the $\tilde{t}$ mass matrix. In the figures below, the assumption $m_{\tilde{q}} \equiv M_{\tilde{t}_L} = M_{\tilde{t}_R}$ is made.

The plot in Fig. 10 shows the result for m_h obtained from the diagrammatic calculation of the full one-loop and leading two-loop contributions. The two steps of refinement discussed above are shown in separate curves. For comparison the pure one-loop result is also given. The results are plotted as a function of $M_t^{LR}/m_{\tilde{q}}$, where $m_{\tilde{q}}$ is fixed to 500 GeV. The qualitative behavior is the same as in [111], where the result containing only the leading one-loop contribution (and without further refinements) was shown. The two-loop contributions give rise to a large reduction of the one-loop result of 10–20 GeV. The two steps of refinement both increase m_h by up to 2 GeV. A minimum occurs for $M_t^{LR} = 0$ GeV which we refer to as 'no mixing' (different from section 1). A maximum in the two-loop result for m_h is reached for about $M_t^{LR}/m_{\tilde{q}} \approx 2$ in the $\tan\beta\ = 1.6$ scenario as well as in the $\tan\beta\ = 40$ scenario. This case we refer to as 'maximal mixing' (differently from section 1). The maximum is shifted compared to its one-loop value of about $M_t^{LR}/m_{\tilde{q}} \approx 2.4$. The two steps of refinement have only a negligible effect on the location of the maximum.

The results of the diagrammatic calculation, including the higher-order terms discussed above, have been implemented into the FORTRAN code *FeynHiggs* [113]; it is available via its WWW-page
`http://www-itp.physik.uni-karlsruhe.de/feynhiggs`.

We now turn to the comparison of the diagrammatic results with the predictions obtained via renormalization group methods. We first compare the diagrammatic result for the no-mixing case, including the refinement terms, with the RG results obtained in [108]. After the inclusion of the refinement terms the diagrammatic result for the no-mixing case agrees very well with the RG result. The deviation

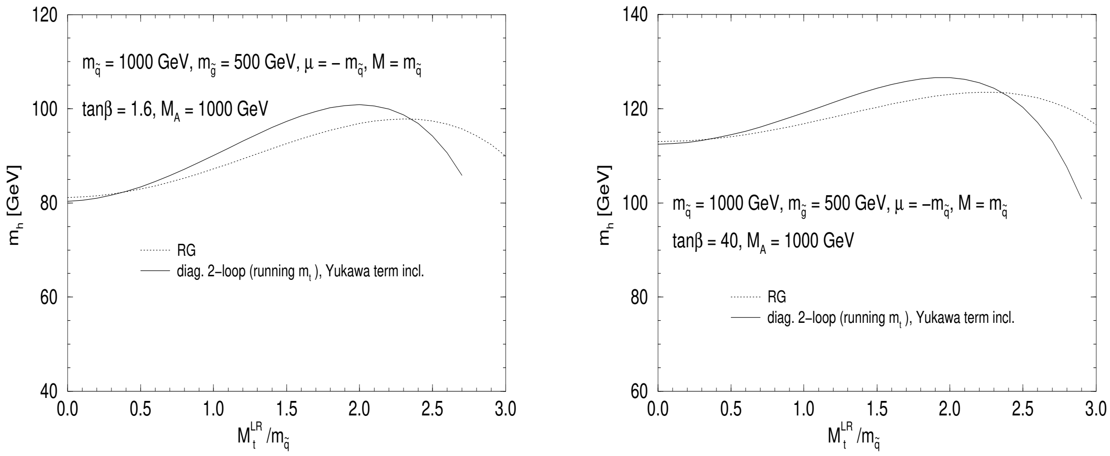

FIGURE 11. Comparison between the Feynman-diagrammatic calculations and the results obtained by renormalization group methods [108]. The mass of the lightest Higgs boson is shown for the two scenarios with $\tan\beta\ = 1.6$ and $\tan\beta\ = 40$ for increasing mixing in the $\tilde{t}$-sector and $m_{\tilde{q}} = M_A$.

between the results exceeds 2 GeV only for $\tan\beta\ = 1.6$ and $m_{\tilde{q}} < 150$ GeV. For smaller values of M_A the comparison for the no-mixing case looks qualitatively the same. For $\tan\beta\ = 1.6$ and values of M_A below 100 GeV slightly larger deviations are possible. Since the RG results do not contain the gluino mass as a parameter, varying $m_{\tilde{g}}$ gives rise to an extra deviation, which in the no-mixing case does not exceed 1 GeV. Varying the other parameters μ and M in general does not lead to a sizable effect in the comparison with the corresponding RG results.

Let us now consider the situation when mixing in the $\tilde{t}$ sector is taken into account. Comparing again the full one-loop result with the one-loop leading-log result used within the RG approach [109] yields good agreement for small mixing (only for values of M_A below 100 GeV and large mixing deviations of about 5 GeV occur). In Fig. 11 the diagrammatic result including the refinement terms is compared with the RG results [108] as a function of $M_t^{LR}/m_{\tilde{q}}$ for $\tan\beta\ = 1.6$ and $\tan\beta\ = 40$. For larger $\tilde{t}$-mixing, sizeable deviations between the diagrammatic and the RG results occur, which can exceed 5 GeV for moderate mixing and become very large for large values of $M_t^{LR}/m_{\tilde{q}}$. As already stressed above, the maximal value for m_h in the diagrammatic approach is reached for $M_t^{LR}/m_{\tilde{q}} \approx 2$, whereas the RG results have a maximum at $M_t^{LR}/m_{\tilde{q}} \approx 2.4$, i.e. at the one-loop value. Varying the value of $m_{\tilde{g}}$ in the Feynman-diagrammatic result leads to a larger effect than in the no-mixing case and shifts the diagrammatic result relative to the RG result within ± 2 GeV.

So far, the results of the diagrammatic on-shell calculation and the RG methods have been compared in terms of the parameters $M_{\tilde{t}_L}$, $M_{\tilde{t}_R}$ and M_t^{LR} of the $\tilde{t}$ mixing matrix, since the available numerical codes for the RG results [108,109] are given in terms of these parameters. However, since the two approaches rely on different renormalization schemes, the meaning of these (non-observable) parameters is not precisely the same in the two approaches starting from two-loop order. Indeed, assuming fixed values for the physical parameters $m_{\tilde{t}_1}$, $m_{\tilde{t}_2}$, $\theta_{\tilde{t}}$ and deriving the corresponding values of the parameters $M_{\tilde{t}_L}$, $M_{\tilde{t}_R}$, M_t^{LR} in the on-shell scheme as well as in the $\overline{MS}$ scheme, sizable differences occur between the values of the mixing parameter M_t^{LR} in the two schemes, while the parameters $M_{\tilde{t}_L}$, $M_{\tilde{t}_R}$ are approximately equal in the two schemes. Thus, part of the different shape of the curves in Fig. 11 may be attributed to a different meaning of the parameter M_t^{LR} in the on-shell scheme and in the RG calculation.

CONCLUSIONS

The experimental data for tests of the standard model have achieved an impressive accuracy. In the meantime, many theoretical contributions have become available to improve and stabilize the standard model predictions and to reach a theoretical accuracy clearly better than 0.1%.

The overall agreement between theory and experiment for the entire set of the precision observables is remarkable and instructively confirms the validity of the standard model. Fluctuations of data around the predictions are within two standard deviations, with no compelling evidence for deviations. Direct and indirect determinations of the top mass are compatible, and a light Higgs boson is clearly favoured by the analysis of precision data in the standard model context, which is far below the mass range where the standard Higgs sector becomes non-perturbative.

As a consequence of the high quality performance of the standard model, any kind of New Physics can only provoke small effects, at most of the size that is set by the radiative corrections. The MSSM, mainly theoretically advocated, is competitive to the standard model in describing the data with about the same quality in global fits. Since the MSSM predicts the existence of a light Higgs boson, the detection of a Higgs at LEP could be an indication of supersymmetry. The standard model can also accommodate such a light Higgs, but with the consequence that its validity cannot be extrapolated to energies much higher than the TeV scale.

ACKNOWLEDGEMENT

I want to express my gratitude to the organizers for the invitation, for the warm hospitality and the enjoyable atmosphere during the VIII Mexican School on Particles and Fields.

REFERENCES

1. The LEP Collaborations ALEPH, DELPHI, L3, OPAL, the LEP Electroweak Working Group and the SLD Heavy Flavor and Electroweak Groups, CERN-PPE/99-15 (1999)
2. D. Karlen, XXIX *International Conference on High Energy Physics*, Vancouver 1998 (to appear in the proceedings)
3. UA2 Collaboration, J. Alitti et al., *Phys. Lett.* B **276**, 354 (1992);
   CDF Collaboration, F. Abe et al., *Phys. Rev. Lett.* **65**, 2243 (1990); *Phys. Rev.* D **43**, 2070 (1991); *Phys. Rev. Lett.* **75**, 11 (1995); *Phys. Rev.* D **52**, 4784 (1995);
   D0 Collaboration, B. Abbott et al., *Phys. Rev. Lett.* **80**, 3008 (1998);
   P. Derwent, A. Kotwal, XXIX *International Conference on High Energy Physics*, Vancouver 1998 (to appear in the proceedings)
4. CDF Collaboration, F. Abe et al., *Phys. Rev. Lett.* **74**, 2626 (1995);
   D0 Collaboration, S. Abachi et al., *Phys. Rev. Lett.* **74**, 2632 (1995)
5. R. Partridge, XXIX *International Conference on High Energy Physics*, Vancouver 1998 (to appear in the proceedings)
6. G. 't Hooft, *Nucl. Phys.* B **33**, 173 (1971) and B **35**, 167 (1971)
7. G. Passarino, M. Veltman, *Nucl. Phys.* B **160**, 151 (1979)
8. M. Consoli, *Nucl. Phys.* B **160**, 208 (1979)
9. A. Sirlin, *Phys. Rev.* D **22**, 971 (1980);
   W. J. Marciano, A. Sirlin, *Phys. Rev.* D **22**, 2695 (1980);
   A. Sirlin, W. J. Marciano, *Nucl. Phys.* B **189**, 442 (1981)
10. D.Yu. Bardin, P.Ch. Christova, O.M. Fedorenko, *Nucl. Phys.* B **175**, 435 (1980) and B **197**, 1 (1982);
    D.Yu. Bardin, M.S. Bilenky, G.V. Mithselmakher, T. Riemann, M. Sachwitz, *Z. Phys.* C **44**, 493 (1989)
11. J. Fleischer, F. Jegerlehner, *Phys. Rev.* D **23**, 2001 (1981)
12. K.I. Aoki, Z. Hioki, R. Kawabe, M. Konuma,
    T. Muta, *Suppl. Prog. Theor. Phys.* **73**,1 (1982);
    Z. Hioki, *Phys. Rev. Lett.* **65**, 683 (1990), E: *ibidem* **65**, 1692 (1990); *Z. Phys.* C **49**, 287 (1991)
13. M. Consoli, S. LoPresti, L. Maiani, *Nucl. Phys.* B **223**, 474 (1983)
14. D.Yu. Bardin, M.S. Bilenky, G.V. Mithselmakher, T. Riemann, M. Sachwitz, *Z. Phys.* C **44**, 493 (1989)
15. M. Böhm, W. Hollik, H. Spiesberger, *Fortschr. Phys.* **34**, 687 (1986)
16. W. Hollik, *Fortschr. Phys.* **38**, 165 (1990)
17. M. Consoli, W. Hollik, F. Jegerlehner, in: *Z Physics at LEP 1*, eds. G. Altarelli, R. Kleiss and C. Verzegnassi, CERN 89-08 (1989)
18. G. Passarino, R. Pittau, *Phys. Lett.* B **228**, 89 (1989);
    V.A. Novikov, L.B. Okun, M.I. Vysotsky, *Nucl. Phys.* B **397**, 35 (1993)
19. G. Passarino, M. Veltman, *Phys. Lett.* B **237**, 537 (1990)
20. W.J. Marciano, A. Sirlin, *Phys. Rev. Lett.* **46**, 163 (1981);
    A. Sirlin, *Phys. Lett.* B **232**, 123 (1989)
21. G. Degrassi, S. Fanchiotti, A. Sirlin, *Nucl. Phys.* B **351**, 49 (1991)

22. G. Degrassi, A. Sirlin, *Nucl. Phys.* B **352**, 342 (1991)
23. M. Veltman, *Phys. Lett.* B **91**, 95 (1980);
M. Green, M. Veltman, *Nucl. Phys.* B **169**, 137 (1980), E: *Nucl. Phys.* B **175**, 547 (1980);
F. Antonelli, M. Consoli, G. Corbo, *Phys. Lett.* B **91**, 90 (1980);
F. Antonelli, M. Consoli, G. Corbo, O. Pellegrino, *Nucl. Phys.* B **183**, 195 (1981)
24. D.C. Kennedy, B.W. Lynn, *Nucl. Phys.* B **322**, 1 (1989)
25. M. Kuroda, G. Moultaka, D. Schildknecht, *Nucl. Phys.* B **350**, 25 (1991)
26. *Reports of the Working Group on Precision Calculations for the Z Resonance*, CERN 95-03 (1995), eds. D. Bardin, W. Hollik, G. Passarino
27. G. Källén, A. Sabry, *K. Dan. Vidensk. Selsk. Mat.-Fys. Medd.* **29** (1955) No. 17
28. M. Steinhauser, *Phys. Lett.* B **429**, 158 (1998)
29. S. Eidelman, F. Jegerlehner, *Z. Phys.* C **67**, 585 (1995)
30. H. Burkhardt, B. Pietrzyk, *Phys. Lett.* B **356**, 398 (1995)
31. M.L. Swartz, *Phys. Rev.* D **53**, 5268 (1996)
32. R. Alemany, M. Davier, A. Höcker, *Eur. Phys. J.* C **2** (1998) 123
33. M. Davier, A. Höcker, *Phys. Lett.* B **419**, 419 (1998); hep-ph/9801361; *Phys. Lett.* B **435**, 427 (1998)
34. A. Höcker, XXIX *International Conference on High Energy Physics*, Vancouver 1998 (to appear in the proceedings)
35. J.H. Kühn, M. Steinhauser, *Phys. Lett.* B **437**, 425 (1998)
36. S. Groote, J. Körner, K. Schilcher, N.F. Nasrallah, *Phys. Lett.* B **440**, 375 (1998)
37. J. Erler, *Phys. Rev.* D **59** 054008 (1999)
38. A.H. Hoang, J.H. Kühn, T. Teubner, *Nucl. Phys.* B **452**, 173 (1995);
K.G. Chetyrkin, J.H. Kühn, M. Steinhauser, *Phys. Lett.* B **371**, 93 (1996); *Nucl. Phys.* B **482**, 213 (1996); B **505**, 40 (1997);
K.G. Chetyrkin, R. Harlander, J.H. Kühn, M. Steinhauser, *Nucl. Phys.* B **503**, 339 (1997)
39. A.D. Martin, D. Zeppenfeld, *Phys. Lett.* B **345**, 558 (1995)
40. E. Braaten, S. Narison, A. Pich, *Nucl. Phys.* B **373** (1992) 581
41. BES Collaboration, Z. Zhan, XXIX *International Conference on High Energy Physics*, Vancouver 1998 (to appear in the proceedings)
42. F. Jegerlehner, DESY 99-007, hep-ph/9901386
43. D. Ross, M. Veltman, *Nucl. Phys.* B **95**, 135 (1975)
44. M. Veltman, *Nucl. Phys.* B **123**, 89 (1977);
M.S. Chanowitz, M.A. Furman, I. Hinchliffe, *Phys. Lett.* B **78**, 285 (1978)
45. J.J. van der Bij, F. Hoogeveen, *Nucl. Phys.* B **283**, 477 (1987)
46. R. Barbieri, M. Beccaria, P. Ciafaloni, G. Curci, A. Vicere, *Phys. Lett.* B **288**, 95 (1992); *Nucl. Phys.* B **409**, 105 (1993);
J. Fleischer, F. Jegerlehner, O.V. Tarasov, *Phys. Lett.* B **319**, 249 (1993)
47. A. Djouadi, C. Verzegnassi, *Phys. Lett.* B **195**, 265 (1987)
48. L. Avdeev, J. Fleischer, S. M. Mikhailov, O. Tarasov, *Phys. Lett.* B **336**, 560 (1994); E: *Phys. Lett.* B **349**, 597 (1995);
K.G. Chetyrkin, J.H. Kühn, M. Steinhauser, *Phys. Lett.* B **351**, 331 (1995)
49. M. Veltman, *Acta Phys. Polon.* B **8**, 475 (1977)

50. J.J. van der Bij, M. Veltman, *Nucl. Phys.* B **231**, 205 (1985)
51. R.E. Behrends, R.J. Finkelstein, A. Sirlin, *Phys. Rev.* **101**, 866 (1956);
T. Kinoshita, A. Sirlin, *Phys. Rev.* **113**, 1652 (1959)
52. T. van Ritbergen, R. Stuart, *Phys. Lett.* B **437**, 201 (1998), *Phys. Rev. Lett.* **82**, 488 (1999)
53. Particle Data Group, C. Caso et al., *Eur. Phys. J. C* **3**, 1 (1998)
54. W.J. Marciano, *Phys. Rev.* D **20**, 274 (1979)
55. M. Consoli, W. Hollik, F. Jegerlehner, *Phys. Lett.* B **227**, 167 (1989)
56. A. Djouadi, *Nuovo Cim.* A **100**, 357 (1988);
D. Yu. Bardin, A.V. Chizhov, Dubna preprint E2-89-525 (1989);
B.A. Kniehl, *Nucl. Phys.* B **347**, 86 (1990);
F. Halzen, B.A. Kniehl, *Nucl. Phys.* B **353**, 567 (1991) 567;
A. Djouadi, P. Gambino, *Phys. Rev.* D **49**, 3499 (1994)
57. B.A. Kniehl, J.H. Kühn, R.G. Stuart, *Phys. Lett.* B **214**, 621 (1988);
B.A. Kniehl, A. Sirlin, *Nucl. Phys.* B **371**, 141 (1992); *Phys. Rev.* D **47**, 883 (1993);
S. Fanchiotti, B.A. Kniehl, A. Sirlin, *Phys. Rev.* D **48**, 307 (1993)
58. K. Chetyrkin, J.H. Kühn, M. Steinhauser, *Phys. Rev. Lett.* **75**, 3394 (1995)
59. A. Sirlin, *Phys. Rev.* D **29**, 89 (1984)
60. G. Degrassi, P. Gambino, A. Vicini, *Phys. Lett.* B **383**, 219 (1996);
G. Degrassi, P. Gambino, A. Sirlin, *Phys. Lett.* B **394**, 188 (1997);
G. Degrassi, P. Gambino, M. Passera, A. Sirlin, *Phys. Lett.* B **418**, 209 (1998)
61. S. Bauberger, G. Weiglein, *Nucl. Instrum. Meth. A* **389**, 318 (1997); *Phys. Lett.* B **419**, 333 (1997)
62. G. Weiglein, *Acta Phys. Polon. B* **29**, 2735 (1998)
63. W. Hollik, B. Krause, A. Stremplat, G. Weiglein, to appear;
A. Stremplat, Diploma Thesis (Karlsruhe 1998)
64. D. Bardin et al., hep-ph/9709229, in: *Reports of the Working Group on Precision Calculations for the Z Resonance*, p. 7, CERN 95-03 (1995), eds. D. Bardin, W. Hollik, G. Passarino
65. G. Degrassi, P. Gambino, A. Sirlin, TUM-HEP-333/98 (to appear), and private communication
66. A.A. Akhundov, D.Yu. Bardin, T. Riemann, *Nucl. Phys.* B **276**, 1 (1986);
W. Beenakker, W. Hollik, *Z. Phys.* C **40**, 141 (1988);
J. Bernabeu, A. Pich, A. Santamaria, *Phys. Lett.* B **200**, 569 (1988)
67. A. Denner, W. Hollik, B. Lampe, *Z. Phys.* C **60**, 193 (1993)
68. K.G. Chetyrkin, A.L. Kataev, F.V. Tkachov, *Phys. Lett.* B **85**, 277 (1979);
M. Dine, J. Sapirstein, *Phys. Rev. Lett.* **43**, 668 (1979);
W. Celmaster, R. Gonsalves, *Phys. Rev. Lett.* **44**, 560 (1980);
S.G. Gorishny, A.L. Kataev, S.A. Larin, *Phys. Lett.* B **259**, 144 (1991);
L.R. Surguladze, M.A. Samuel, *Phys. Rev. Lett.* **66**, 560 (1991);
A. Kataev, *Phys. Lett.* B **287**, 209 (1992)
69. K.G. Chetyrkin, J.H. Kühn, *Phys. Lett.* B **248**, 359 (1990) and B **406**, 102 (1997);
K.G. Chetyrkin, J.H. Kühn, A. Kwiatkowski, *Phys. Lett.* B **282**, 221 (1992);
K.G. Chetyrkin, A. Kwiatkowski, *Phys. Lett.* B **305**, 285 (1993) and B **319**, 307 (1993)

70. B.A. Kniehl, J.H. Kühn, *Phys. Lett.* B **224**, 229 (1990); *Nucl. Phys.* B **329**, 547 (1990);
K.G. Chetyrkin, J.H. Kühn, *Phys. Lett.* B **307**, 127 (1993);
S. Larin, T. van Ritbergen, J.A.M. Vermaseren, *Phys. Lett.* B **320**, 159 (1994);
K.G. Chetyrkin, O.V. Tarasov, *Phys. Lett.* B **327**, 114 (1994)
71. K.G. Chetyrkin, J.H. Kühn, A. Kwiatkowski, in *Reports of the Working Group on Precision Calculations for the Z Resonance*, p. 175, CERN 95-03 (1995), eds. D. Bardin, W. Hollik, G. Passarino;
K.G. Chetyrkin, J.H. Kühn, A. Kwiatkowski, *Phys. Rep.* **277**, 189 (1996)
72. J. Fleischer, F. Jegerlehner, P. Rączka, O.V. Tarasov, *Phys. Lett.* B **293**, 437 (1992);
G. Buchalla, A.J. Buras, *Nucl. Phys.* B **398**, 285 (1993);
G. Degrassi, *Nucl. Phys.* B **407**, 271 (1993);
K.G. Chetyrkin, A. Kwiatkowski, M. Steinhauser, *Mod. Phys. Lett.* A **8**, 2785 (1993)
73. A. Kwiatkowski, M. Steinhauser, *Phys. Lett.* B **344**, 359 (1995);
S. Peris, A. Santamaria, *Nucl. Phys.* B **445**, 252 (1995)
74. R. Harlander, T. Seidensticker, M. Steinhauser, *Phys. Lett.* B **426**, 125 (1998)
75. A. Czarnecki, J.H. Kühn, *Phys. Rev. Lett.* **77**, 3955 (1996); E: **80**, 893 (1998)
76. A. Hoang, J.H. Kühn, T. Teubner, *Nucl. Phys.* B **455**, 3 (1995); **452**, 173 (1995)
77. SLD Collaboration, S. Fahey, XXIX *International Conference on High Energy Physics*, Vancouver 1998 (to appear in the proceedings)
78. P. Gambino, A. Sirlin, *Phys. Rev. Lett.* **73**, 621 (1994)
79. NuTev Collaboration, T. Bolton, XXIX *International Conference on High Energy Physics*, Vancouver 1998 (to appear in the proceedings)
80. D. Bardin et al., hep-ph/9412201
81. G. Montagna, O. Nicrosini, F. Piccinini, G. Passarino, hep-ph/9804211
82. D. Bardin, G. Passarino, hep-ph/9803425;
D. Bardin, M. Grünewald, G. Passarino, hep-ph/9902452
83. J. Erler, P. Langacker, hep-ph/9809352; hep-ph/9801422
84. K. Hagiwara, D. Haidt, S. Matsumoto, *Eur. Phys. J.* C **2**, 95 (1998);
J. Ellis, G.L. Fogli, E. Lisi, *Phys. Lett.* B **389**, 321 (1996); *Z. Phys.* C **69**, 627 (1996);
G. Passarino, *Acta Phys. Polon.* **28**, 635 (1997);
S. Dittmaier, D. Schildknecht, *Phys. Lett.* B **391**, 420 (1997);
S. Dittmaier, D. Schildknecht, G. Weiglein, *Phys. Lett.* B **386**, 247 (1996);
P. Chankowski, S. Pokorski, *Acta Phys. Polon.* **27**, 1719 (1996)
85. W. de Boer, A. Dabelstein, W. Hollik, W. Mösle, U. Schwickerath, *Z. Phys.* C **75**, 627 (1997)
86. D. Treille, XXIX *International Conference on High Energy Physics*, Vancouver 1998 (to appear in the proceedings)
87. L. Maiani, G. Parisi, R. Petronzio, *Nucl. Phys.* B **136**, 115 (1979);
N. Cabibbo, L. Maiani, G. Parisi, R. Petronzio, *Nucl. Phys.* B **158**, 259 (1979);
R. Dashen, H. Neuberger, *Phys. Rev. Lett.* **50**, 1897 (1983);
D.J.E. Callaway, *Nucl. Phys.* B **233**, 189;
M.A. Beg, C. Panagiotakopoulos, A. Sirlin, *Phys. Rev. Lett.* **52**, 883 (1984);

M. Lindner, *Z. Phys.* C **31**, 295 (1986)
88. M. Lindner, M. Sher, H. Zaglauer, *Phys. Lett.* B **228**, 139 (1989);
G. Altarelli, G. Isidori, *Phys. Lett.* B **337**,141 (1994);
J.A. Casas, J.R. Espinosa, M. Quiros, *Phys. Lett.* B **342**, 171 (1995) and B **382**, 374 (1996);
89. T. Hambye, K. Riesselmann, *Phys. Rev.* D **55**, 7255 (1997)
90. Kuti et al., *Phys. Rev. Lett.* **61**, 678 (1988);
P. Hasenfratz et al., *Nucl. Phys.* B **317**, 81 (1989);
M. Lüscher, P. Weisz, *Nucl. Phys.* B **318**, 705 (1989);
M. Göckeler, H. Kastrup, T. Neuhaus, F. Zimmermann, *Nucl. Phys.* B **404**, 517 (1993)
91. M. Göckeler, H. Kastrup, J. Westphalen, F. Zimmermann, *Nucl. Phys.* B **425**, 413 (1994)
92. A. Ghinculov, *Nucl. Phys.* B **455**, 21 (1995);
A. Frink, B. Kniehl, K. Riesselmann, *Phys. Rev.* D **54**, 4548 (1996)
93. T. Binoth, A. Ghinculov, J.J. van der Bij, *Phys. Rev.* D **57**, 1487 (1998); *Phys. Lett.* B **417**, 343 (1998)
94. L. Durand, B.A. Kniehl, K. Riesselmann, *Phys. Rev. Lett.* **72**, 2534 (1994); E: *ibidem* B **74**, 1699 (1995);
A. Ghinculov, *Phys. Lett.* B **337**, 137 (1994); E: *ibidem* B **346**, 426 (1995);
V. Borodulin, G. Jikia, *Phys. Lett.* B **391**, 434 (1997)
95. K. Riesselmann, hep-ph/9711456
96. A. Denner, R. Guth, W. Hollik, J.H. Kühn, *Z. Phys.* C **51**, 695 (1991);
J. Rosiek, *Phys. Lett.* B **252**, 135 (1990;
M. Boulware, D. Finnell, *Phys. Rev.* D **44**, 2054 (1991)
97. G. Altarelli, R. Barbieri, F. Caravaglios, *Phys. Lett.* B **314**, 357 (1993);
C.S. Lee, B.Q. Hu, J.H. Yang, Z.Y. Fang, *J. Phys.* G **19**, 13 (1993);
Q. Hu, J.M. Yang, C.S. Li, *Commun. Theor. Phys.* **20**, 213 (1993);
J.D. Wells, C. Kolda, G.L. Kane, *Phys. Lett.* B **338**, 219 (1994);
G.L. Kane, R.G. Stuart, J.D. Wells, *Phys. Lett.* B **354**, 350 (1995);
M. Drees et al., *Phys. Rev.* D **54**, 5598 (1996)
98. P. Chankowski, A. Dabelstein, W. Hollik, W. Mösle, S. Pokorski, J. Rosiek, *Nucl. Phys.* B **417**, 101 (1994);
D. Garcia, J. Solà, *Mod. Phys. Lett.* A **9**, 211 (1994)
99. D. Garcia, R. Jiménez, J. Solà, *Phys. Lett.* B **347**, 309 and 321 (1995);
D. Garcia, J. Solà, *Phys. Lett.* B **357**, 349 (1995);
A. Dabelstein, W. Hollik, W. Mösle, in *Perspectives for Electroweak Interactions in e^+e^- Collisions*, Ringberg Castle 1995, ed. B.A. Kniehl, World Scientific 1995 (p. 345);
P. Chankowski, S. Pokorski, *Nucl. Phys.* B **475**, 3 (1996)
100. A. Djouadi, P. Gambino, S. Heinemeyer, W. Hollik, C. Jünger, G. Weiglein, *Phys. Rev. Lett.* **78**, 3626 (1997); *Phys. Rev.* D **57**, 4179 (1998)
101. J. Erler, D. Pierce, *Nucl. Phys.* B **526**, 53 (1998)
102. H. Haber, R. Hempfling, *Phys. Rev. Lett.* **66**, 1815 (1991);
Y. Okada, M. Yamaguchi, T. Yanagida, *Prog. Theor. Phys.* **85**, 1 (1991);

J. Ellis, G. Ridolfi, F. Zwirner, *Phys. Lett.* B **257**, 83 (1991) and B **262**, 477 (1991); R. Barbieri, M. Frigeni, *Phys. Lett.* B **258**, 395 (1991)
103. P. Chankowski, S. Pokorski, J. Rosiek, *Nucl. Phys.* B **423**, 437 (1994)
104. A. Dabelstein, *Nucl. Phys.* B **456**, 25 (1995); *Z. Phys.* C **67**, 495 (1995)
105. J. Bagger, K. Matchev, D. Pierce, R. Zhang, *Nucl. Phys.* B **491**, 3 (1997)
106. J. Casas, J. Espinosa, M. Quirós, A. Riotto, *Nucl. Phys.* B **436**, 3 (1995), E: *ibid.* B **439**, 466 (1995)
107. M. Carena, J. Espinosa, M. Quirós, C. Wagner, *Phys. Lett.* B **355**, 209 (1995)
108. M. Carena, M. Quirós, C. Wagner, *Nucl. Phys.* B **461**, 407 (1996)
109. H. Haber, R. Hempfling, A. Hoang, *Z. Phys.* C **75**, 539 (1997)
110. R. Hempfling, A. Hoang, *Phys. Lett.* B **331**, 99 (1994)
111. S. Heinemeyer, W. Hollik, G. Weiglein, *Phys. Rev.* D **58**, 091701 (1998)
112. S. Heinemeyer, W. Hollik, G. Weiglein, *Phys. Lett.* B **440**, 296 (1998)
113. S. Heinemeyer, W. Hollik, G. Weiglein, hep-ph/9812320